

Astronomical Tests of General Relativity and the Pseudo-Complex Theory

Thomas Boller and Andreas Müller

Abstract Gravitation is very well described by Einstein's General Relativity. However, several theoretical predictions like the existence of curvature singularities and event horizons are under debate. This motivated to modify the standard theory of gravity. Here, we contrast predictions made by General Relativity with the pseudo-complex field theory proposed recently. Among them we study the gravitational redshift effect, perihelion shift, orbital motion, timing measurements and spectral lines. We consider supermassive black holes as ideal testbeds to test the theoretical predictions in the regime of strong gravity. In particular, we investigate the innermost centers of active galaxies and the Galactic Centre. This involves high-performance astronomical instruments of the next generation. We present feasibility studies with the proposed Athena X-ray experiment and with the upcoming GRAVITY near-infrared instrument to be mounted at the Very Large Telescope.

1 Introduction

Gravitation is successfully described by Einstein's General Relativity (GR) invented 100 years ago. The success of GR consists in an impressive number of experimental tests and by now GR passes them all. We use GR to describe the spacetime of our Earth and meanwhile GR effects are daily business in navigation systems. Einstein's theory also adequately describes massive bodies like our Sun or even more massive and compact objects like stellar mass black holes and neutron stars which are endpoints of stellar evolution as well as supermassive black holes. A breakthrough was certainly

T. Boller (✉)

Max Planck-Institute for extraterrestrial physics, PSF 1312, 85741 Garching, Germany
e-mail: bol@mpe.mpg.de

A. Müller

Technische Universität München, Excellence Cluster Universe, 85741 Garching, Germany
e-mail: andreas.mueller@universe-cluster.de

the description of our whole Universe by GR. The Friedmann cosmology successfully describes the dynamics of our Universe.

However, some mysteries remain in the framework of GR, such as the appearance of curvature singularities and event horizons. This motivated some scientists to go beyond GR. Since the advent of GR many other, alternative gravitational theories have been developed. Early after Einstein's publication of General Relativity in 1916, alternative theories of gravitation entered the stage. Some of them involved at least one more spatial extra dimension like the Kaluza-Klein theory or string theory. Others involve a different ansatz for the Einstein tensor, the left-hand side of Einstein's field equation, like $f(R)$ gravity which assumes a more general curvature expression for the Einstein tensor. A new ansatz is called pseudo-complex field theory [1] which goes in a similar direction as the latter one.

Interestingly, it is astronomy which offers a zoo of cosmic objects to test the strong gravity effects predicted by GR. Here, we confront these predictions of the standard GR picture with the predictions given by the pseudo-complex theory. We are lucky enough to find significant differences which allow to discriminate between the two theories. As we will see, these tests involve especially cosmic black holes. If we want to probe the strong gravity of black holes we have to get very close to these beasts. Therefore, these studies naturally involve (but not only) X-ray astronomy because X-rays are the signals coming from the immediate black hole surroundings. We will show what will be observational signatures accessible by X-ray telescopes and also by infrared instruments of the next generation of modern astronomical instruments.

2 Gravitational Theories

In this section we first sketch two gravitational theories, General Relativity in Sect. 2.1, and the pseudo-complex field theory proposed recently in Sect. 2.2.

2.1 *Einstein's General Relativity*

Albert Einstein published a new theory for gravity in 1915. It is called General Relativity (GR) and is a completely different ansatz to describe gravity than Newtonian gravity. The Newtonian forces are no longer existent. Gravity is described by a four-manifold, a four dimensional continuum of space and time: spacetime. This is the dynamical stage for matter and for light. In Special Relativity, spacetime is flat and is described by the Minkowski metric. In GR, the spacetime is generally curved. The sources for gravity are any type of energy E and according to $E = mc^2$ also by mass m . The speed of light, c , is a fundamental constant in this framework. Its concrete value is not given by theory and has to be measured by experiments.

The fundamental field equation in GR involves more complicated mathematical objects called tensors. The essential statement of GR is that matter and energy curves

spacetime, and spacetime dictates matter and light where to move. The tracks along which particles and light move are called geodesics and GR allows to extract a geodesics equations for each given metric. The field equation of GR holds simply $G = T$ (ignoring any constants and indices) whereas G is the Einstein tensor containing curvature and T is the stress-energy tensor containing energy and mass. In more detail the field equation of GR looks like this

$$R^{\mu\nu} - \frac{1}{2}g^{\mu\nu}R = \frac{8\pi\kappa}{c^2}T^{\mu\nu}, \quad (1)$$

where $R^{\mu\nu}$ denotes the Ricci tensor (a contraction of the Riemann tensor) and R is the Ricci scalar. κ is the coupling constant of gravity which according to the correspondence principle is proportional to Newton's constant. This equation is very powerful, but also very complicated. Written in its whole beauty it is a coupled system of ten partial and non-linear differential equations. Mathematics cannot provide a full set of solutions for equations of this kind. Therefore, theorists found again and again new special solutions for the field equations of GR.

The two most important solutions in the context of this work are the Schwarzschild solution and the Kerr solution. The (outer) Schwarzschild solution was found by Karl Schwarzschild in 1916 [2] and describes a point mass in GR. The Schwarzschild spacetime is spherically symmetric and static. The Kerr solution was found in 1963 (significantly later!) by Roy Kerr [3] and describes a rotating mass in GR. The Kerr spacetime is axially symmetric and stationary. Both spacetimes describe cosmic black holes. They only have very few parameters ("No-hair theorem"). A Schwarzschild black hole has only mass M and a Kerr black hole has mass M and angular momentum J . Usually theorists use the specific angular momentum, $a = J/M$.

It is now the task of astronomers to find cosmic sources where black holes could be present. Then, it would be interesting to develop methods to measure the black hole parameters M and a by observations.

2.2 The Pseudo-Complex Theory

A new formulation of a field theory for gravity, based on a pseudo-complex description has been first published by [1]. An update of the pseudo-complex theory is given by [5]. Here, we only sketch the ansatz. A pseudo-complex number X can be written as:

$$X = X_R + I \times X_I, \quad \text{with } I^2 = +1. \quad (2)$$

From this a new Einstein equation follows and can be formulated as

$$R^{\mu\nu} - \frac{1}{2}g^{\mu\nu}R = \frac{8\pi\kappa}{c^2}T^{\mu\nu}\sigma_- \quad \text{with } \sigma_- = \frac{1}{2}(1-I), \quad \sigma_-\sigma_+ = 0 \quad \sigma_-^2 = \sigma_- \quad (3)$$

where the energy-stress tensor represents a field with repulsive properties (c.f. [5] for a detailed description). A comparison of this new field equation with Eq. 1 shows just one more additional quantity on the right. σ_- is called zero divisor basis. The authors mentioned above deduced a new metric tensor from the new Einstein equations. Its 00 component satisfies:

$$g_{00} = \frac{r^2 - 2Mr + a^2 \cos^2(\theta) + \frac{B}{2r}}{r^2 + a^2 \cos^2(\theta)} \quad (4)$$

with a as introduced before and an integration constant B .

Here, we use the gravitational radius $R_G = GM/c^2$ with black hole mass M , Newton's constant G and vacuum speed of light c . An interesting new feature in pseudo-complex field theory is that it removes the coordinate singularity at the Schwarzschild radius $r = 2 R_G \equiv R_S$, which is a prediction of GR. Interestingly, there is therefore also no event horizon. This means that a classical black hole is absolutely dark at the horizon whereas a pseudo-complex black hole is rather gray, i.e. light originating at this region might escape to an external observer. We will return to this aspect in Sect. 3.

3 Predictions and Tests of General Relativity Versus the Pseudo-Complex Field Theory

In this section we work out several tests for General Relativity and confront them with those of the pseudo-complex field theory. We propose to test the innermost stable circular orbit (Sect. 3.1), the gravitational redshift (Sect. 3.2), perihelion shift (Sect. 3.3), timing studies (Sect. 3.4) and, the profile of relativistic emission lines (Sect. 3.5).

We note that experimental tests of the pseudo-complex theory have also been published by [4].

3.1 Comparison of the Effective Potentials and Innermost Stable Orbits

In classical mechanics potentials are tools to investigate the motion of point masses. In celestial mechanics, astronomers use the gravitational potential in Newtonian gravity to study e.g. the motion of planets around the Sun. Effective potentials are suitable approaches in GR to study the orbital motion of test particles.

The effective potential obtained from the pseudo-complex theory differs from that obtained in the standard GR as we show in Fig. 1 taken from [5]. The effective potential of classical black holes can be found in the literature, e.g. [6].

In both plots the curves are parametrized by the angular momentum, L , of the orbiting test particle. The relative minima of the curves correspond to stable Kepler

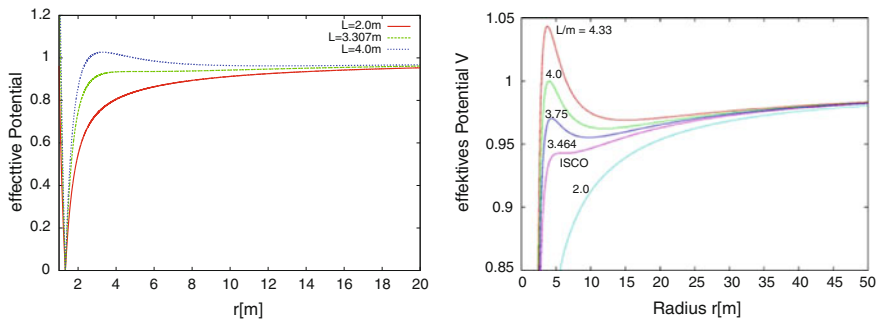


Fig. 1 *Left panel:* effective potential as a function of radius in the pseudo-complex theory for a black hole spin of $a = 0$ (plot adopted from [5]). The *green curve* shows a reversal point at $5.3 R_G$ which defines the ISCO. The ISCO is different from the standard theory. Below $4/3 R_G$ the effective potential is increasing, corresponding to repulsion as described in Sect. 2.2. *Right panel:* effective potential in the standard GR for $a = 0$ (plot taken from [7]). The ISCO is located at $6 R_G$

orbits. The absolute minima indicate the infall into the central mass concentration. The innermost stable circular orbit (ISCO) is defined by the reversal point, i.e. the second derivative is equal to zero.

A common method in X-ray astronomy is to determine the ISCO from observations and to link it to a spin value as explained by theory. GR essentially says: The closer the stable orbit, the higher the spin. The ISCO varies from $9 R_G$ ($a = -M$, retrograde) over $6 R_G$ ($a = 0$) to $1 R_G$ ($a = M$, prograde).

Now, the left panel of Fig. 1 shows the effective potential for the pseudo-complex theory. The ISCO is at $5.3 R_G$ in the pseudo-complex theory, which is below $6.0 R_G$ where the ISCO of a non-spinning black hole with $a = 0$ is located. Here we see that, as a consequence, the spin determination is different between the two theories. This allows to discriminate between the two gravitational theories.

Pseudo-complex field theory exhibits another interesting feature. This is shown in the left panel of Fig. 1. Moving further inwards, we see that the effective potential is increasing again very steeply at a distance less than $4/3 R_G$. It looks like a repulsion which is similar to the Yukawa potential in nuclear physics. This region sits deep in the black hole, too close to be feasible with current observational techniques. But maybe this might be tested in the future.

The orbital motion around black holes will be tested to unprecedented accuracy with a new infrared instrument at ESO's Very Large Telescope (VLT) in Chile. This detector of the forthcoming second generation of Very Large Telescope Interferometry (VLTI) instrumentation is called GRAVITY. GRAVITY will provide astrometric measurements with a precision of the order of one Schwarzschild radius, $R_S = 2 GM/c^2$, of the black hole Sgr A* in the centre of the Milky Way [8]. The GRAVITY project will allow to probe physics in the strong field limit (c.f. Sect. 3.3 and Sect. 3.4) and will revolutionize measurements of motions of stellar orbits in the Galactic Centre. A summary of the whole science cases and the instrument capabilities are given in [9].

3.2 Gravitational Redshift Near Black Holes

Gravitational redshift characterizes the effect that light is trapped by a gravitational source, i.e. a mass. The influence on radiation is twofold: first, the energy of the photons is shifted towards lower energies, i.e. to the red end of the spectrum. Hence, it is a redshift. Second, the effect influences the spectral flux, i.e. it lowers the observed intensity. Gravitational redshift dims the light. The gravitational redshift effect is omnipresent for any mass and a prediction by any metric gravitational theory, therefore also for GR. For black holes this effect is extraordinarily strong. A black hole is in a sense defined by this effect because it exhibits an event horizon which marks the region where any local emission is reduced to zero as observed externally.

The Schwarzschild radius $R_S = 2 GM/c^2$ only depends on the mass parameter, i.e. the more massive the black hole the larger it will appear from the outside. However, the distance plays a role. The more distant the black hole, the smaller its event horizon region will appear. This apparent size, θ_{BH} , can be easily computed from black hole mass M and its distance d and satisfies

$$\theta_{\text{BH}} = 39.4 \times \frac{M}{10^6 M_{\odot}} \times \frac{1 \text{ kpc}}{d} \mu\text{arcsec}, \quad (5)$$

where $M_{\odot} = 2 \times 10^{33} \text{ g}$ denotes the mass of the Sun, 1 kpc = 3260 light years is a common distance unit, and $1 \mu\text{arcsec} = 10^{-6} \text{ arcsec}$. Plugging in the values for the Galactic Centre black hole ($M_{\text{GC}} = 4 \times 10^6 M_{\odot}$, $d_{\text{GC}} = 8 \text{ kpc}$) [10] and M87, the massive elliptical galaxy in the Virgo Cluster ($M_{\text{M87}} = 6 \times 10^9 M_{\odot}$, $d_{\text{M87}} = 16 \text{ Mpc}$) delivers $\theta_{\text{BH, GC}} = 20 \mu\text{arcsec}$ and $\theta_{\text{BH, M87}} = 15 \mu\text{arcsec}$ which is remarkably similar. The M87 supermassive black hole is significantly more massive but also significantly more distant.

So, these are the apparent sizes of the two black holes at the sky. They are very tiny, compared e.g. to the apparent size of the full moon, $\theta_{\text{Moon}} = 0.5^{\circ} = 1800 \text{ arcsec} = 1.8 \times 10^9 \mu\text{arcsec}$. However, modern interferometric techniques are capable to resolve such tiny regions. Among them are Very Long Baseline Interferometry (VLBI) in radio astronomy (e.g. [11–13]) and the GRAVITY instrument [14, 15]. GRAVITY has sufficient resolution to test the gravitational redshift effect in the Galactic Centre as well as in the extragalactic source M87. However, the darkening towards the black hole is in GR different from the pseudo-complex theory as shown in Fig. 2. We expect that the observations with GRAVITY will be good enough to discriminate between GR and the pseudo-complex field theory at the innermost few gravitational radii.

Not only the Galactic Centre host a supermassive black hole, they are also present in other galaxies, most probably in all galaxy centres—sometimes even more than one massive black hole. One particular class is different from the centre of the Milky Way because the luminosity is very high. Astrophysicists call them active galactic nuclei (AGN), i.e. the luminous cores of galaxies powered by an accreting supermassive black hole. There are various AGN families, e.g. Seyfert galaxies which are rather

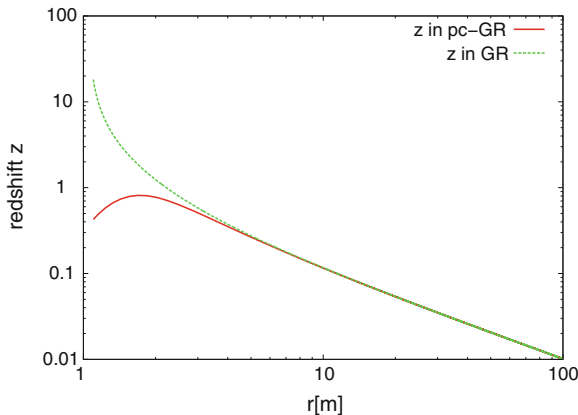


Fig. 2 Gravitational redshift as a function of R_G for the pseudo-complex theory (*green curve*) and the standard theory (*red curve*) for a black hole spin of $a = 0.998$. The figure has been adopted from [5]

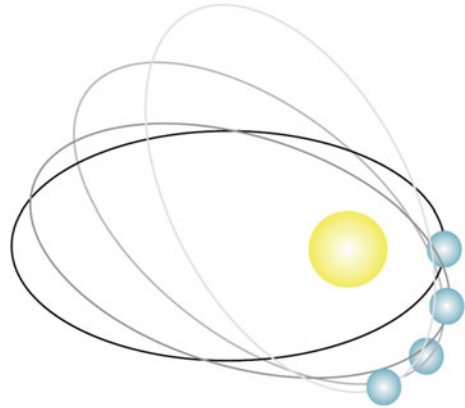
low in luminosity and quasars which are very luminous. According to a common geometrical model there are two AGN types. AGN type-1 are seen face-on, i.e. the observer on Earth looks into the AGN core. AGN type-2 are rather seen edge-on, i.e. the observer cannot look into the AGN core. The view is blocked by a giant and massive dust torus sitting at large radii. We are dealing here with a special AGN type called Narrow-line Seyfert 1 (NLS1) which belongs to the AGN type-1.

In X-ray bright AGN, it is assumed that most of the X-ray emission is arising within only a few R_G and that the central emission is highly peaked with emissivity indices of about 6, e.g. [16, 17]. The future Athena mission will provide even more precise measurements in many other AGNs [18]. Athena is a large mission candidate of ESA's Cosmic Vision program 2015-2025. The main science objectives of Athena are to (i) explore the extreme physical conditions around black holes, (ii) map the large scale structure of the universe, and (iii) study the physics of feedback on all astrophysical scales. Significant differences between the ratio of the observed intensities arise from both theories. Assuming that most of the emission is arising at $1.2 R_G$, the gravitational redshift z_G is about 0.7 in the pseudo-complex theory and about 6 in the standard theory for a Kerr black hole (c.f. Fig. 2). This translates into generalized Doppler factors [19] $g = 1/(1 + z_G)$ of 0.6 and 0.14 for the pseudo-complex and the standard theory, respectively. As the observed and rest frame intensities scale according to the Liouville theorem with

$$I_v^{\text{obs}} = g^3 \times I_v^{\text{rest}}. \quad (6)$$

the ratio of the observed intensities between the pseudo-complex and the standard theory is about 70 assuming a Kerr black hole. As a consequence pseudo-complex black holes are brighter than standard GR black holes. With the Athena X-ray satellite measurements in the immediate vicinity around many black holes will become much more precise and this will allow to test different gravitational theories.

Fig. 3 Sketch which illustrates the perihelion shift, i.e. the motion of the complete orbit of a celestial body. This was observed for the innermost planet Mercury orbiting the Sun



3.3 Perihelion Shifts

With the advent of GR, first tests were proposed already in the second decade of the 20th Century. One observational fact remained unexplained so far, namely the the motion of Mercury’s orbit. Since the the 19th Century, Mercury’s orbit has been known with much more accuracy. At that time, the French astronomer Urbain Le Verrier used Mercury’s transits to track the orbits very precisely. In particular, the so-called perihelion shift¹ represented a mystery. This phenomenon is shown in Fig. 3. Mercury’s as the closest planet to the Sun shows a remarkably large perihelion shift amount. This phenomenon is also present in the classical Newtonian gravitational theory. However, the observations did not match the Newtonian prediction. A discrepancy of 43 arcsec remained unexplained. Einstein’s General Relativity did this perfect match and hence the triumphal procession of GR started one hundred years ago.

Meanwhile, the performance of astronomical instruments increased significantly. Today, it is possible to track perihelion shift beyond the solar system, i.e. in the centre of the Milky Way. Here, the GRAVITY experiment comes into play again. The GRAVITY experiment in its astrometric mode will allow to precisely track the motion of stars around the supermassive black hole in Sgr A* with an accuracy of 10 μ arcsec (c.f. [14, 15]). Based on simulations of the stellar orbits, the authors show in their Fig. 2 that GRAVITY will probe radial precession and even the Lense-Thirring effect (“frame-dragging”). This brings us to another test already present in GR: frame-dragging. This is an effect where the rotating spacetime drags any test particle and also light. However, this effect decays steeply as moving away from the gravitational rotating source. For a rotating black hole classically described by the Kerr metric, the rotation of spacetime (i.e the gradient of frame dragging frequency) decays with the third power of the distance. Therefore, astronomers have to get close

¹ Perihelion denotes the point on the orbit closest to the Sun.

to the gravitational rotating source, which means that the spatial resolution has to be high. This is what GRAVITY can perform.

Recently, the frame-dragging effect for the rotating Earth was observed with the experiments LAGEOS and Gravity Probe B. Here, the positions of satellites were accurately under control by the use of lasers. The gyroscopes onboard these missions were sensitive enough to test the rotation of Earth's spacetime. Perihelion and frame dragging effects are the classical tests for the standard theory and GRAVITY will allow test field theories in the strong gravity limit. Currently, the concrete results in the pseudo-complex field theory are work in progress. As soon as they are available they could be tested against the standard GR picture.

3.4 Keplerian Motion and Timing Analyses

The planets in the solar system move on Keplerian orbits. The classical Keplerian laws can be proven by using Newtonian gravity. With the advent of GR, these laws have to be modified to apply them to relativistic bodies such as black holes. However, in a moderate distance to the black hole the good old Keplerian laws apply. This is the case for one of the innermost stars orbiting the central massive black hole in the Milky Way, close to the radio source Sgr A* in the constellation Sagittarius (Sgr). Astronomers were able to track the complete orbit for the star S2 [20]. The 3rd Keplerian law states

$$\frac{\tau^2}{a^3} = \frac{4\pi^2}{GM} = \text{const}, \quad (7)$$

with the orbital time τ , the length of the semi-major axis a , Newton's constant G and the central mass M .

In fact, τ and a are observables at Sgr A* by means of infrared observations, e.g. with observations at the VLT or with Keck on Hawaii. This delivered the high mass concentration in the heart of the Milky Way. Approximately 4 million solar masses in a region comparable with the solar system in size. The best interpretation for the compact object sitting there is the one of a classical massive black hole described by GR.

Quasi-periodic frequencies of infrared and X-ray emission have been detected in the Galactic Centre as well as in a few active galaxies. Usually, this is interpreted as modulated emission coming from orbiting hot spots [15] report on quasi-periodic frequencies of this kind in the Galactic Centre which exhibit a time scale of about 20–22 min (c.f. their Fig. 2). Such quasi-periodic frequencies can be compared with the prediction of Keplerian frequencies from the standard and the pseudo-complex theory. In Fig. 4 we show the Keplerian frequencies as a function of the distance to the black hole for both theories, calculated for a mass of 4.3×10^6 solar masses and a black hole spin of $a = 0.995$. The lower limit for the black hole spin in the Galactic Center is 0.52 [10]. Assuming that the black hole spin of the supermassive black hole in the Galactic Centre is determined with forthcoming GRAVITY and Athena observations, the Keplerian frequencies shown in Fig. 4 for the standard and the

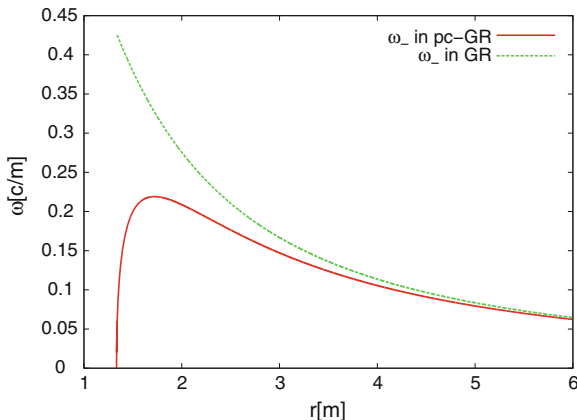


Fig. 4 Keplerian frequencies as a function of the distance to a black hole with a mass of $M = 4.3 \times 10^6$ solar masses and a black hole spin of $a = 0.995$. The plot has been adopted from [5]

pseudo-complex theory can be directly compared. We note that at distances smaller than about $2 R_G$ there occur significant differences between both theories. The same holds for the quasi-periodic oscillations detected in AGNs (c.f. Fig. 5).

Matter which is infalling into a black hole emits significant amounts of high-energetic X-rays. Typically, bright and hot emission features form, so-called hot spots. They orbit the black hole a few times and finally the black hole swallows the clump. Temperature inhomogeneities in the accretion disc, often referred to as X-ray hot spots, are expected to produce a special signature of the Fe $K\alpha$ line emission in the energy-time plane. Figure 5 taken from [21] shows the smoothed theoretical time-energy map of emission features from an orbiting flare observed in the Seyfert galaxy NGC 3516. It could be shown that the feature varies systematically in flux at intervals of 25 ks. The peak moves in energy between 5.7 and 6.5 keV. The spectral evolution of the feature agrees with Fe K emission arising from a spot on the accretion disc, illuminated by a co-rotating flare located at a radius of (7-16) R_G , modulated by Doppler and gravitational effects as the flare orbits around the black hole.

Astronomers who would like to observe this phenomena caught-in-the-act need X-ray telescopes with a high time-resolution. Time-resolved X-ray spectroscopy with Athena is a technique to follow X-ray emission features of this kind. Such observations will allow to test different theories of the strong gravity limit. While approaching the black hole the emission is characteristically influenced by the dynamics, but also by the curved spacetime of the black hole. A first effect is the relativistic version of the Doppler effect. Relativistic Doppler boosting beams the emission towards the observer while the orbiter is approaching along the line of sight. As a consequence, the emission is shifted to higher energies and is brighter than in the rest frame (Doppler blueshift). On the receding side of the orbital track the emission is beamed away from the observer. Hence, the emission is shifted to lower energies

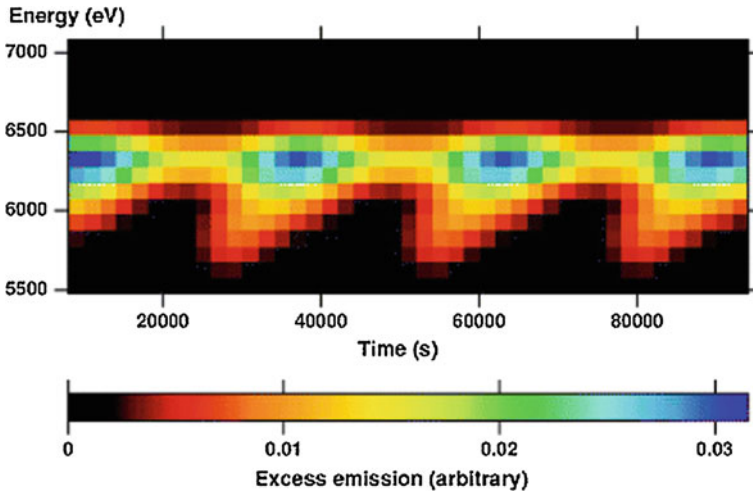


Fig. 5 Smoothed theoretical time-energy map of emission features from an orbiting flare in NGC 3516. The Doppler effect produces the characteristic sinusoidal variations. The period is determined by the orbital time scale

and is dimmer than in the rest frame (Doppler redshift). If the orbital plane should be oriented in a face-on manner then only the quadratic Doppler effect survives.

In addition to this dynamical effect, we have a black hole sitting close by the orbiter. Its highly curved space-time drags the light and causes the relativistic gravitational redshift effect. The presence of the black hole's deep gravitational potential hinders the light from escaping—at least the light which comes to close to the hole. At some critical surface called the event horizon nothing can escape the black hole. This is where the emission dies out and the black hole itself becomes visible as an (like GR says) absolutely dark spheroidal zone. This stands in contrast to the background which has some brightness, e.g. from the surrounding accretion flow or, if there is no accretion, at least from the ambient cosmic microwave background radiation.

3.5 Relativistic Emission Line Studies

One prominent X-ray feature is the iron $K\alpha$ line at 6.4 keV rest frame energy. This spectral line is produced by a fluorescence process. Electrons are excited into a higher state on the L shell and decay either by emitting an Auger electron (66 % probability), or by the emission of a fluorescence photon with 6.4 keV while the electron drops from the L to K shell (33 % probability). Typically a spectral line is rather sharp in the rest frame and can be sufficiently modeled by a narrow Gaussian profile. However, in the observer's frame the spectral line is distorted by the aforementioned relativistic Doppler and gravitational redshift effects. In the astronomical context

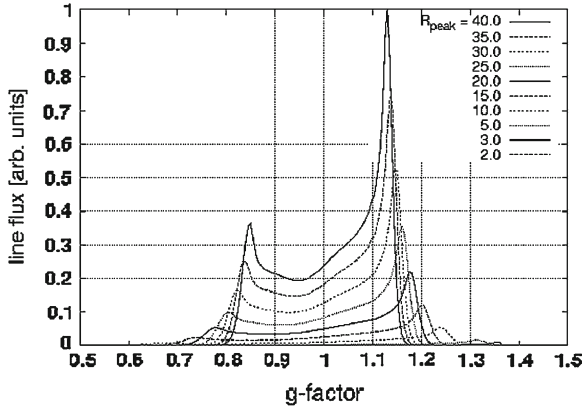


Fig. 6 Decay of a relativistic line profile as a function of an emission region approaching the black hole. Due to the gravitation redshift effect the line profile becomes broader and gets dimmer (Image taken from [23])

the iron K line is produced in hot accretion disks around stellar and supermassive black hole. Astronomers observe a typical line profile which is coming from low to intermediately inclined accretion disks, e.g. active galaxies of type-1. In total, the observed fluorescent iron K lines for these sources are typically broad, skew with a long smeared red tail on the red line wing due to gravitational redshift and a peaked beamed blue wing due to Doppler blueshift.

The relativistic ray tracing technique is a standard method in relativistic astrophysics to visualize GR effects and to simulate relativistically broadened line profiles, see e.g. [19, 22]. Figure 6 [23] illustrates how the line profile decays as the emission region approaches the black hole. R_{Peak} is the radius where the emission of the ring is maximal, given in units of gravitational radii R_G . Due to the gravitation redshift effect the line profiles broadens and gets dimmer and vanishes finally.

Relativistic line profiles from infalling hot spots.

The analysis is based on the theoretical model presented by [24]. The authors assume that the 6keV line features are due to localized spots which occur on the surface of an accretion disk around a Schwarzschild black hole. They presented simulated line profiles as a function of orbital phase of the spot and its radial distance to the black hole. The models predict a specific behavior of the light curves and of the variability in the energy-time plane. In the model the hot spot starts at $5.6 R_G$, slightly below the marginally stable orbit (at $6 R_G$ for a Schwarzschild black hole) and disappears at the horizon at $2 R_G$, i.e the Schwarzschild radius. The infall time corresponds to roughly 1.6 orbits which correspond to 30ks for a black hole with 50 million solar masses. The size of the spot is $0.25 R_G$. The trajectory of the hot spot, the spectrum in the energy-time plane, and the unfolded spectra for several infall segments as shown in Fig. 7.

Feasibility studies of infall motion for the Athena instrument.

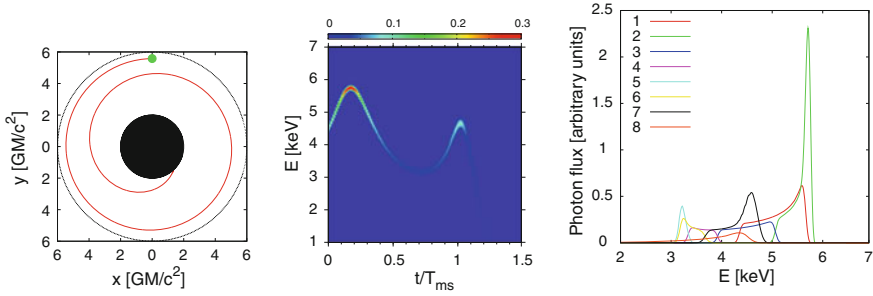


Fig. 7 *Left* The trajectory of the hot spot is depicted by the red, the spot size is colored in green. The central black hole is the black hole region surrounded by the marginally stable. *Middle* The dynamics of the Fe $K\alpha$ emission line in the energy-time plane. The time is given in units of Keplerian orbital time at the ISCO. The mid panel shows the subsequent die out of the line due to gravitational redshift of an orbiter approaching more and more to the black hole. *Right* The model spectra for time bins 1 to 8 while the infall time is divided into 10 bins. The photon flux for time bins 9 and 10 is very low, i.e. invisible in the plot

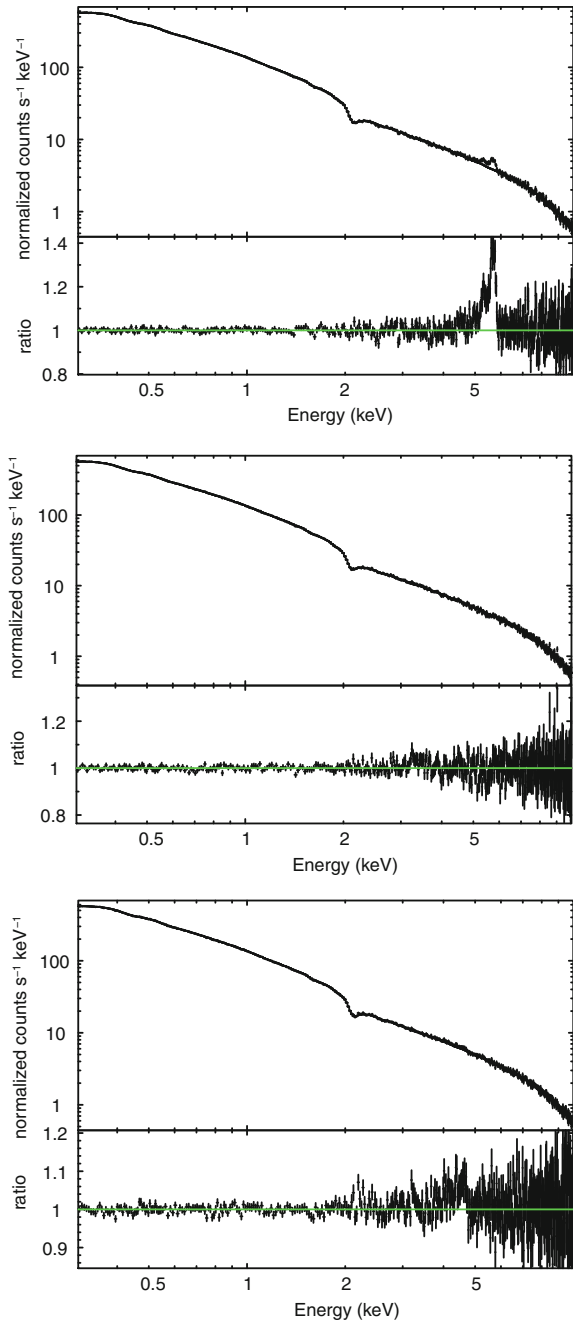
Now, we link the infall model to concrete X-ray observations with Athena [18]. We have folded the 5 time segments of the infalling hot spot with the model parameters described above with the Athena Wide Field Imager [25] response. In Fig. 8 we show, that the signature of the infalling hot spot shows off and on phases so that even the duration of the non-detections give important information about the kinematics and timescale of the infalling material. As the gravitational redshift and the Kepler frequencies are different at small distances to the black hole for standard and the pseudo-complex theory (c.f. Figs. 2 and 4), significant differences are expected for the Fe K line profiles and the infall frequencies, which can be measured and tested with Athena.

Here we have shown the expected effects based on Einstein’s GR theory. The theoretical calculation of the relativistic line profiles and infall times for the pseudo-complex theory is currently under investigation. Quantitative results for relativistic line studies for the the pseudo-complex theory will be reported elsewhere. The theoretical and consequently the observed line profiles and infall times will significantly differ from Einsteins GR theory and will provide another important test for both theories.

4 Astronomical Observations of Active Galaxies

In this section we summarize astronomical observations which serve as the basis for the proposed tests of General Relativity and its pseudo-complex extension.

Fig. 8 Simulation of Athena observations. *Left* first infall segment: the residuals are clearly visible due to the Doppler boosting. This can be considered as the Athena on-phase of the detection of the infalling spot. The second infall segment is not plotted, as the line profile becomes undetectable due to smearing in a large range of energies and so buried in the continuum. *Middle* Third infall segment: At this stage, the spot is receding from the observer. Doppler boosting creates a red peak around 3 keV which is not visible in the data because the relative contribution of the line is smaller whereas more flux is coming from the continuum. The statistics is too poor to detect relativistic line emission. *Right* fourth infall segment: interestingly, the relativistic line profile becomes visible again, at late infall times and at distances very close to the black hole. This is due to Doppler boosting (beaming). However, the line core is now shifted to lower energies around 4.5 keV, because gravitational redshift is getting stronger. For the final stages of the infall the gravitational redshift effect is too strong to reveal relativistic signatures



4.1 Previous Research Work

The fact that accretion onto black holes powers the most luminous sources in the Universe is known for decades ([26–28]). Pioneering work on flaring emission near black holes was performed by [29]. First work on relativistic light curves of a star orbiting a black hole was done by [30]. One breakthrough was the detection of relativistic broad emission lines which are emitted on an accretion disk by fluorescence of hard X-ray radiation. In this way, radiation from a nearby primary hard X-ray source, called corona, is reprocessed. The dominant line feature is produced by iron which has the largest fluorescence yield among all elements. The core of the broad iron $K\alpha$ line can be found at a rest frame energy of 6.4 keV and line fits revealed that it originates only a few gravitational radii away from the black hole. This feature is visible in several AGN (e.g. [31–33]) and galactic black hole candidates (e.g. [34]). Reverberation mapping studies exploit the physics between the first power-law continuum flare emission and the lagging emission line response. In this way, one can constrain the position of the flare emitter and the spacetime (black hole spin), see e.g. [35, 36]. The flare could be linked to the disk and therefore orbit with the disk or it could be a stationary emitter on the disk rotational axis, e.g. the jet base. A detailed understanding of this geometry is still lacking.

4.2 Present X-ray Observations Near Black Holes

4.2.1 Spectral Analysis

Observations with XMM-Newton, Chandra and Suzaku revealed that the inner accretion flows around black holes emit significant amounts of X-rays. Both X-ray spectra and the time variability of this X-ray emission contain a wealth of information about the innermost matter flow and the black hole itself. Over the last decades, many X-ray observations of stellar black holes in X-ray binaries and supermassive black holes in active galactic nuclei delivered insights into the black hole-accretion flow system. It is possible to fit, e.g. temperature of the accretion flow, inclination angle of the disk towards the observer, disk emissivities as well as mass and spin of the black hole. The radiation originates so close to the black hole that it allows for probing the dynamics of matter and the interactions between matter and radiation in the strong gravity limit. X-ray astronomers have found that the primary X-ray emission is concentrated solely to the central part of the accretion disc and must lie within 1 gravitational radius of the event horizon of the black hole. This was convincingly shown by [16] for X-ray observations in the narrow-line Seyfert 1 galaxy 1H 0707-495 in its low flux state.

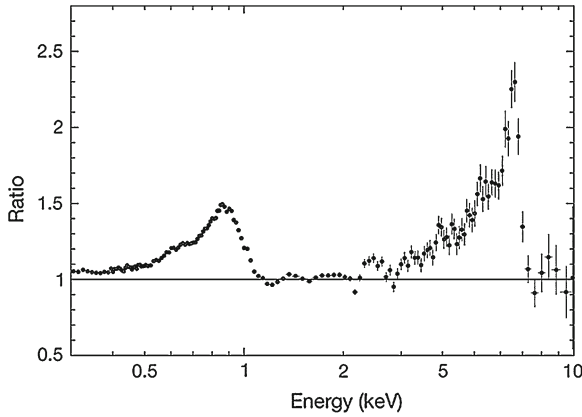


Fig. 9 The first detection of both Fe K and Fe L line emission in the NLS1 1H 0707-495. The ratio of the normalization of the Fe K to the Fe L line in photon flux is 20 to 1, in agreement to atomic physics. The Fe L line becomes most probably detectable due to the high Fe abundance which is about 9 times higher than in the solar environment ([37])

4.2.2 Timing Analysis

Signatures of X-ray hot spots orbiting a supermassive black hole have been detected in a few AGN (c.f. Sect. 3.4 and Fig. 5). These observations are based on the observed Fe $K\alpha$ emission as a function of time and allows to constrain the distance of the X-ray hot spots to the central black hole.

Cross-correlation analyses of time series from different spectral bands yield further insight into the intertwined physical processes of the accretion disc. They certainly have a great discovery potential — as it was impressively demonstrated by the detection of the reverberation signature, namely the detection of time lags between the Fe K and L line (c.f. Figs. 9, 10 and its physical interpretation [37]). The Fe K and L line emission is caused by X-ray fluorescence at the return of an electron of iron of the L to the K-shell after excitation of the iron with an X-ray photon, i.e. the Fe K line emission is caused by the return of an electron to the K shell, and the Fe L emission is due to the return of an electron to the L shell. Relativistic distortion of the line makes it sensitive to the strong gravity and spin of the black hole. The normalization of the Fe K and Fe L lines in photon spectra are in the ratio 20 to 1—in agreement to atomic physics. The bright iron L emission allows the detection of a reverberation lag of about 30s between the direct X-ray continuum and its reflection from matter falling into the black hole.

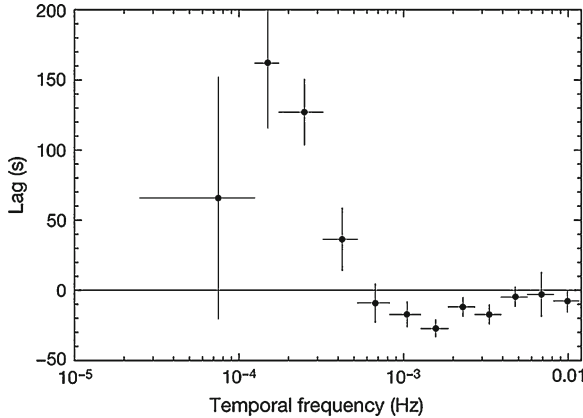


Fig. 10 Detection of a frequency dependent time lag of 1H 0707-495. The soft band is defined in the energy range between 0.3 and 1.0 keV, the hard band between 1.0 and 4.0 keV. A positive time lag indicates that the hard band follows the soft band, opposite to negative time lags. At the lowest frequencies positive time lags are detected. These are interpreted as accretion rate fluctuations at larger distances to the black hole. A significant negative time lag lag has been detected at 30 s. This is interpreted as the detection of a reverberation lag

4.3 Future X-ray Observations

We have shown that present X-ray missions are very successful in delivering data from inner accretion flows near black holes. So far, the accretion onto black holes is a paradigm to power luminous X-ray sources, however detailed timing studies of the infalling matter are still lacking. Furthermore, the event horizon of a black hole was not proven observationally so far. One may put doubts whether or not an observational proof by means of electromagnetic waves is possible. So far, there are a few standard methods for determining black hole spin. However, various techniques contradict to each other which might be a hint that either the model or even the theory is wrong. The proposed Athena satellite mission will bring important new results from the innermost matter flow around black holes and we expect essential new insight into the nature of gravity.

5 Summary

Einstein's General Relativity is the best theory we currently have to describe gravitational effects. However, it is a non-quantized theory and the interesting question is whether or not there are regimes where we have to go beyond Einstein's Relativity. Do curvature singularities in black holes really exist in nature, or do they signal a problem? And what about event horizons? There are also a product of GR but never

have been proven so far. The regime of strong gravity is very fascinating in this context because it offers an opportunity to get answers to this interesting questions.

Here, we confront standard GR with a new suggestion for a gravitational theory which is called pseudo-complex field theory. We elaborated test examples which enable us to test strong gravity and to discriminate between GR and the alternative pseudo-complex theory. So far, the tests involve in particular gravitational redshift and Keplerian motion. We also presented an outlook on how further tests could look like. They involve perihelion shifts of close orbiting particles, orbital motions of matter around supermassive black holes as well as X-ray timing and spectral analyses. This is work in progress and we have just shown a preview. The detailed results will be discussed elsewhere.

The ideal experimental objects to test the theoretical predictions are places where black holes harbor. These is the Galactic Centre and some very suited active galaxies. These astronomical testbeds will be our targets to test strong gravity. These tests involve instruments which are not yet available. We need high-performance detectors to come as close as possible to the black holes. We selected two proposals of forthcoming instruments of the next generation, namely Athena, an ESA X-ray mission, and GRAVITY, an instrument mounted at ESO's Very Large Telescope in Chile. With both high-performance instruments we expect to be able to learn more about the nature of gravity in its strong regime.

Acknowledgments TB and AM greatly acknowledge extensive scientific discussions with P. Hess, W. Greiner, T. Schönembach and G. Caspar on the topics presented in this paper. TB is much obliged to W. Greiner for his longstanding scientific support. We thank M. Dovciak and J. Svoboda from the Astronomical Institute of the Academy of Science in Prag, Czech Republic, who significantly contributed in writing up Sect. 3.5. TB is grateful to S. Gillessen for intense discussion on the Galactic Center research.

References

1. P.O. Hess, W. Greiner, Pseudo-complex general relativity. *Int. J. Mod. Phys. E* **18**, 51–77 (2009)
2. K. Schwarzschild, Über das Gravitationsfeld eines Massenpunktes nach der Einsteinschen Theorie. *Sitzungsber. Preuss. Akad. Wiss. Berlin (Math.Phys.)*, 189–196 (1916)
3. R.P. Kerr, Gravitational field of a spinning mass as an example of algebraically special metrics. *Phys. Rev. Lett.* **11**, 237 (1963)
4. G. Caspar et al., Pseudo-complex general relativity: Schwarzschild, Reissner-Nordström and Kerr solutions. *Int. J. Mod. Phys. E* **21**(1250015), 1–39 (2012)
5. T. Schönembach, G. Caspar, P.O. Hess, T. Boller, A. Müller, M. Schäfer, W. Greiner, Experimental tests of pseudo-complex General relativity, arXiv:1209.2815 [gr-qc] (2012)
6. M. Camenzind, *Compact Objects in Astrophysics: White Dwarfs Neutron Stars and Black Holes* (Springer, New York, 2007)
7. A. Mueller, www.astronomiewissen.de.
8. F.H. Vincent et al., in *The Galactic Center: A Window to the Nuclear Environment of Disk Galaxies*, ed. by M.R. Morris, Q.D. Wang, F. Yuan. Proceedings of a workshop held at Shanghai, China, 19–23 Oct 2009. (Astronomical Society of the Pacific, San Francisco, 2011), p. 275
9. F. Eisenhauer et al., GRAVITY: observing the universe in motion. *The Messenger* **143**, 16–24 (2011)

10. R. Genzel et al., Near-infrared flares from accreting gas around the supermassive black hole at the Galactic Centre. *Nature* **425**, 934 (2003)
11. V.L. Fish et al., 1.3 mm wavelength VLBI of Sagittarius A*: detection of time-variable emission on event horizon scales. *ApJ* **727**, 36 (2011)
12. R.S. Lu et al., Multiwavelength VLBI observations of Sagittarius A*. *A&A* **525**, 76 (2011)
13. S. Doeleman et al., Imaging an event horizon: submm-VLBI of a super massive black hole (2012), <http://de.arxiv.org/abs/0906.3899>
14. F.H. Vincent et al., Performance of astrometric detection of a hotspot orbiting on the innermost stable circular orbit of the Galactic Centre black hole. *MNRAS* **412**, 653 (2011)
15. F. Eisenhauer et al., GRAVITY: getting to the event horizon of Sgr A*. *SPIE* **7013**, 69 (2008)
16. A.C. Fabian et al., 1H 0707–495 in 2011: an X-ray source within a gravitational radius of the event horizon. *MNRAS* **419**, 116 (2012)
17. Th. Boller, in *Soft X-ray reflection and strong and weak field limit determination in Narrow-Line Seyfert 1 Galaxies, Exploring Fundamental Issues in Nuclear Physics*, ed. by D. Bandyopadhyay. Proceedings of the Symposium on Advances in Nuclear Physics in Our Time, (World Scientific Publishing Co. Pte. Ltd., 2012) ISBN-13 978–981–4355–72–8
18. K. Nandra, ATHENA: The advanced telescope for high energy astrophysics, the X-ray Universe 2011, Presentations of the conference held in Berlin, Germany, 27–30 June 2011. Available online at: <http://xmm.esac.esa.int/external/>, article id.022, 2011
19. A. Müller, M. Camenzind, Relativistic emission lines from accreting black holes. The effect of disk truncation on line profiles. *A&A* **413**, 861 (2004)
20. S. Gillessen et al., The orbit of the star S2 around SGR A* from very large telescope and keck data. *ApJ* **707**, L114 (2009)
21. K. Iwasawa et al., Flux and energy modulation of redshifted iron emission in NGC 3516: implications for the black hole mass. *MNRAS* **355**, 1073 (2004)
22. A.C. Fabian et al., X-ray reflection in the narrow-line Seyfert 1 galaxy 1H 0707–495. *MNRAS* **353**, 1071 (2004)
23. A. Müller, M. Wold, On the signatures of gravitational redshift: the onset of relativistic emission lines. *A&A* **457**, 485 (2006)
24. M. Dovciak et al., Relativistic spectral features from X-ray-illuminated spots and the measure of the black hole mass in active galactic nuclei. *MNRAS* **350**, 745 (2004)
25. L. Strüder et al., The wide-field imager for IXO: status and future activities. *SPIE* **7732**, 46 (2010)
26. Y.B. Zel'dovich, I.D. Novikov, The radiation of gravity waves by bodies moving in the field of a collapsing star. *Sov. Phys. Dokl.* **9**, 246 (1964)
27. E.E. Salpeter, Accretion of interstellar matter by massive objects. *ApJ* **140**, 796 (1964)
28. D. Lynden-Bell, Galactic nuclei as collapsed old quasars. *Nature* **223**, 690 (1969)
29. J.M. Bardeen et al., Rotating black holes: locally nonrotating frames, energy extraction, and scalar synchrotron radiation. *ApJ* **178**, 347 (1972)
30. C.T. Cunningham, J.M. Bardeen, The Optical Appearance of a Star Orbiting an Extreme Kerr Black Hole. *ApJ* **183**, 237 (1973)
31. Y. Tanaka et al., Gravitationally redshifted emission implying an accretion disk and massive black hole in the active galaxy MCG-6-30-15. *Nature* **375**, 659 (1995)
32. A.C. Fabian, K. Iwasawa, Broad Fe-K lines from Seyfert galaxies. *Adv. Space Res.* **25**, 471–480 (2000)
33. K. Nandra et al., An XMM-Newton survey of broad iron lines in Seyfert galaxies. *MNRAS* **382**, 194 (2007)
34. J.M. Miller et al., in *Relativistic Iron Lines in Galactic Black Holes: Recent Results and Lines in the ASCA Archive, The Tenth Marcel Grossmann Meeting* ed. by Mário Novello; Santiago Perez Bergliaffa; Remo Ruffini. Proceedings of the MG10 Meeting held at Brazilian Center for Research in Physics (CBPF), Rio de Janeiro, Brazil, 20–26 July 2003. Singapore: World Scientific Publishing, in 3 volumes, ISBN 981-256-6678 (set), ISBN 981-256-980-4 (Part A), ISBN 981-256-979-0 (Part B), ISBN 981-256-978-2 (Part C), 2005, XLVIII + 2492 p.: 2005, p. 1296, 2005

35. C.S. Reynolds, in *Compton Reflection and Iron Fluorescence in Active Galactic Nuclei and Galactic Black Hole Candidates, High Energy Processes in Accreting Black Holes*, ed. by J. Poutanen, R. Svensson. ASP Conference Series 161, ISBN 1-886733-81-3 (1999), p. 178 (1999)
36. A.J. Young, C.S. Reynolds, Iron line reverberation mapping with constellation-X. *ApJ* **529**, 101 (2000)
37. A.C. Fabian et al., Broad line emission from iron K- and L-shell transitions in the active galaxy 1H0707-495. *Nature* **459**, 540 (2009)